Journal of Biotechnology 141 (2009) 137–141

Contents lists available at ScienceDirect

Journal of Biotechnology

journal homepage: www.elsevier.com/locate/jbiotec

Investigation of the unfolding pathway of *Bacillus thuringiensis* Cyt2Aa2 toxin reveals an unfolding intermediate

Anchanee Sangcharoen[a], Weerachon Tepanant[a], Somruathai Kidsanguan[a], Boonhiang Promdonkoy[b], Chartchai Krittanai[a,*]

[a] *Institute of Molecular Biology and Genetics, Mahidol University, Salaya Campus, Putthamonthon 4 Road, Salaya, Nakhonpathom 73170, Thailand*
[b] *National Center for Genetic Engineering and Biotechnology (BIOTEC), National Science and Technology Development Agency, 113 Phahonyothin Road, Klong 1, Klong Luang, Pathumthani 12120, Thailand*

ARTICLE INFO

Article history:
Received 1 November 2008
Received in revised form 4 March 2009
Accepted 16 March 2009

Keywords:
Cyt2Aa2
Bacillus thuringiensis
Protein unfolding
Molten globule
Intrinsic fluorescence
Circular dichroism

ABSTRACT

Cyt2Aa2 is a cytolytic toxin from *Bacillus thuringiensis* subsp. *darmstadiensis*. Its active form has a lethal activity against specific mosquito larvae. We characterized an unfolding pathway of Cyt2Aa2 using a guanidinium hydrochloride denaturation. The results revealed three-state transition with a detectable intermediate in a condition with 3–4 M of GuHCl. The conformational free energies for native and intermediate state unfolding were 5.82 ± 0.47 and 16.85 ± 1.47 kcal/mol, respectively. Kinetic analysis suggested that the activation energy of both transitions was around 23–25 kcal/mol, with a rate-limiting step in the second transition. These results have established an energy profile of the Cyt2Aa2 toxin in various conformations involved in the unfolding/refolding pathway. Further characterization of the intermediate state by dye-binding assay, intrinsic fluorescence, and circular dichroism spectroscopy demonstrated characteristics of a molten globule state. This revealed intermediate could play an active role in the structural folding and biological activity of the toxin.

1. Introduction

Bacillus thuringiensis is a spore-forming, Gram-positive soil bacterium which produces parasporal proteins during sporulation (Nickerson et al., 1975). The produced endotoxins can be solubilized in alkaline pH, and become insecticidal after proteolysis by insect gut proteases (Murphy et al., 1976; Bulla et al., 1977; Andrews et al., 1985; Armstrong et al., 1985). The binding of an active toxin on the brush border membrane of a susceptible insect could result in the formation of ion channels or pores, leading to osmotic imbalance, cell swelling and osmotic lysis (Hofte and Whiteley, 1989; Schnepf et al., 1998).

The cytolytic toxin Cyt2Aa2 is produced by *B. thuringiensis* subsp. *darmstadiensis* (Promdonkoy et al., 2003). This toxin is synthesized as a 29-kDa protoxin and then proteolytically processed into a 25-kDa active form. Its toxicity is found against *Stegomyia* and *Culex* sp. mosquito larvae (Galjart et al., 1987). The X-ray structure of Cyt2 toxin contains a single domain of α/β architecture comprising six α-helices and seven β-sheets (Li et al., 1996). Cyt toxin can bind and form pores in a synthetic lipid membrane without the requirement of a receptor (Thomas and Ellar, 1983). The precise mechanism of action for Cyt toxin is still unclear, and may be based on either pore-forming (Promdonkoy and Ellar, 2000, 2003) or detergent-like model (Butko, 2003). To study the details of membrane interaction, stable conformational states of the toxin should be identified and characterized. The present study aims to analyze the conformational states of Cyt2Aa2 toxin using a chemically induced unfolding experiment. The identified conformational states and calculated transitional free energy between each state in the unfolding pathway could help reveal an energy map of the toxin. In addition, the stable intermediate state can also be characterized further to provide a clue to its possible involvement in the structural folding and biological function of Cyt2Aa2 toxin.

2. Materials and methods

2.1. Protein expression and purification

Cyt2Aa2 protein was expressed at 37 °C in *Escherichia coli* strain JM 109 (Promdonkoy et al., 2003) in the presence of 0.1 mM IPTG. The culture media was LB broth containing 100-μg/ml ampicillin. The cell culture was disrupted using a French pressure cell. The harvested inclusion protein was solubilized in 50 mM carbonate buffer (pH 10.0). The soluble toxin was then chromatographically purified using a Superdex-200 HR10/30 size-exclusion column (Amersham). Protein concentration was determined based

* Corresponding author. Tel.: +662 800 3624x1410; fax: +662 441 9906.
E-mail address: stckt@mahidol.ac.th (C. Krittanai).

0168-1656/$ – see front matter © 2009 Elsevier B.V. All rights reserved.
doi:10.1016/j.jbiotec.2009.03.012

on Bradford dye-binding assay and far-UV absorption (Waddell, 1956).

2.2. Circular dichroism spectroscopy

CD spectra were obtained by a Jasco J-715 spectropolarimeter, purged with oxygen-free nitrogen (Jasco, Japan). The instrument was calibrated daily with 1.0 mg/ml (+)-10-camphorsulphonic acid (CSA), yielding an intensity ratio between 192 and 290 nm greater than 2.0. A sample of 0.4–0.6 mg/ml was loaded into a cylindrical quartz cuvette of 0.02-cm path length (Hellma, USA) and analyzed from 190 to 260 nm. Scanning was set at a rate of 20 nm/min, with 1.0-s response time, 50-millidegree sensitivity and four accumulations. All spectra were subtracted by baseline spectra of buffers containing an appropriate concentration of GuHCl.

2.3. Intrinsic fluorescence spectroscopy

Emission spectra were monitored from 300 to 500 nm on Jasco FP-6300 and Perkin Elmer LS-50B spectrofluorometers, based on an excitation of intrinsic fluorescence from aromatic side chains at 280 nm. Samples containing 20–40 μg/ml of protein were analyzed in a rectangular quartz cuvette of 0.5-cm path length. Scanning rate was 50 nm/min. At least three repetitive scans were obtained and averaged.

2.4. Steady-state unfolding

A series of GuHCl stock from 0 to 6.0 M was freshly prepared and used to unfold the protein at 4 °C. The purified toxin was incubated overnight in various concentrations of GuHCl, and then monitored for conformational state by fluorescence spectroscopy. An accurate concentration of GuHCl in each individual condition was confirmed by a refractive index, as described by Nozaki (1972). An unfolding curve of the toxin was constructed from a fluorescence intensity ratio between 330 and 350 nm ($F_{330/350}$). The observed spectral intensity (I_{obs}) was fitted by the three-state equation:

$$I_{obs} = \frac{I_N + I_I\,(\exp\,(m_{NI}[C]\text{-}m_{NI}[C]^{NI\ 50\%})/RT) + I_U\{(\exp\,(m_{NI}[C]\text{-}m_{NI}[C]^{NI\ 50\%})/RT) \times (\exp\,(m_{IU}[C]\text{-}m_{IU}[C]^{IU\ 50\%})/RT)\}}{1+(\exp\,(m_{NI}[C]\text{-}m_{NI}[C]^{NI\ 50\%})/RT) + \{(\exp\,(m_{NI}[C]\text{-}m_{NI}[C]^{NI\ 50\%})/RT) \times (\exp\,(m_{IU}[C]\text{-}m_{IU}[C]^{IU\ 50\%})/RT)\}}$$

$I_N = \alpha_N + \beta_N[C]$, $I_I = \alpha_I + \beta_I[C]$, and $I_U = \alpha_U + \beta_U[C]$

where I_N, I_I and I_U are the intensity for N, I and U states; α and β are Y-intercepts and slopes of these states; and [C] is the GuHCl concentration. The transitional midpoint $[C]^{50\%}$ and unfolding free energy of the protein in the absence of denaturant $\Delta G^{\circ}_{w} = m[C]^{50\%}$ at 25 °C were obtained by curve fitting (Ibarra-Molero and Sanchez-Ruiz, 1996).

2.5. Kinetic unfolding

The toxin (20–40 μg/ml) was mixed with various concentrations of GuHCl. The fluorescence spectra decay was recorded at 340 nm over a time course from 2000 to 5000 s, using an excitation wavelength of 280 nm. The bandwidths of excitation and emission were 5 nm. The fluorescence decay spectra were subtracted by baseline spectra obtained in the first 50 s. Each curve was then fitted to the first order single exponential equation (using the SigmaPlot 6.0 software suite):

$$I_t = I_\alpha + \Delta I \exp^{(-k_{obs})t}$$

where I_t is the signal intensity at a given time, I_α is the signal intensity at the plateau, I_0 is the initial intensity, ΔI is the difference of I_α and I_0, k_{obs} is the kinetic rate constant (which is denaturant dependent), and t is time. The $\ln k_{obs}$ was plotted against the GuHCl concentration and fitted with the linear equation

$$\ln k_{obs} = m[\text{GuHCl}] + \ln k_w$$

where $\ln k_w$ is the natural log of the kinetic rate constant in water, m is the slope, and [GuHCl] is the concentration of GuHCl. The k_w value was used for the activation energy calculation

$$k_w = \left(\frac{k_B T}{h}\right) \exp^{(-E_{ac,w})/RT}$$

where k_B is Boltzmann's constant (1.3807×10^{-23} J/K), h is Planck's constant (6.6261×10^{-34} m^2 kg/s), T is absolute temperature (K), R is the gas constant (1.987 cal/mol K) and $E_{ac,w}$ is the activation energy.

2.6. ANS binding assay

1-Anilino-8-naphthalene-sulfonate (ANS) was applied to determine the conformational state of an unfolding intermediate. Cyt2Aa2 protoxin (30 μg/ml) was incubated in various concentrations of GuHCl for 16–18 h. ANS was then added to a final concentration of 100 μM, mixed and incubated for 5 min in the dark. The samples were scanned for emission spectra from 420 to 600 nm at an excitation wavelength of 350 nm. Slit width for excitation and emission spectra was 5 nm. The spectra of blank solution (without protein) were recorded for subtraction. Intensity changes at a particular wavelength (465 nm) versus GuHCl concentrations were documented.

3. Results and discussion

3.1. Steady-state unfolding and transitional free energy analysis

We employed intrinsic fluorescence spectroscopy to monitor for conformational states of Cyt2Aa2 in various GuHCl concentrations. The toxin in an initial condition of carbonate buffer gave a fluorescence emission spectrum with λ_{max} around 330 nm. When the denaturant was gradually increased in the unfolding condition, the spectra progressively changed, with a reduction of emission

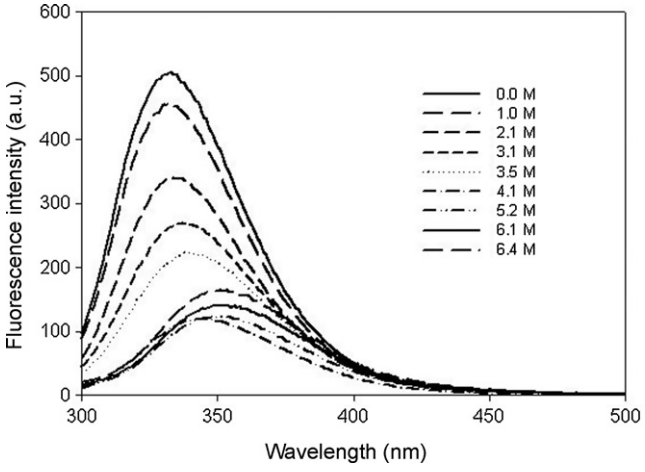

Fig. 1. Intrinsic fluorescence spectra of Cyt2Aa2 toxin in various concentrations of guanidinium hydrochloride. Purified toxin of 20–40 μg/ml was incubated overnight in 0.0–6.4 M GuHCl. The emission spectra were obtained from 300 to 500 nm, with an excitation at 280 nm.

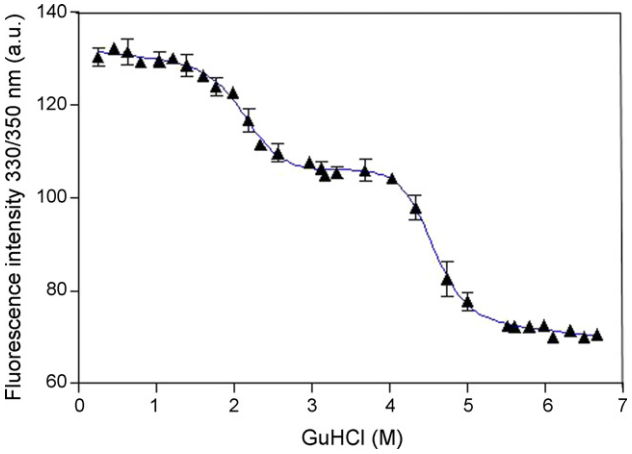

Fig. 2. An unfolding curve of Cyt2Aa2 toxin derived from a plot of the fluorescence intensity ratio for native (N) and unfolded (U) states between 330 and 350 nm, respectively. The three-state transition model was demonstrated to be a function of the denaturant.

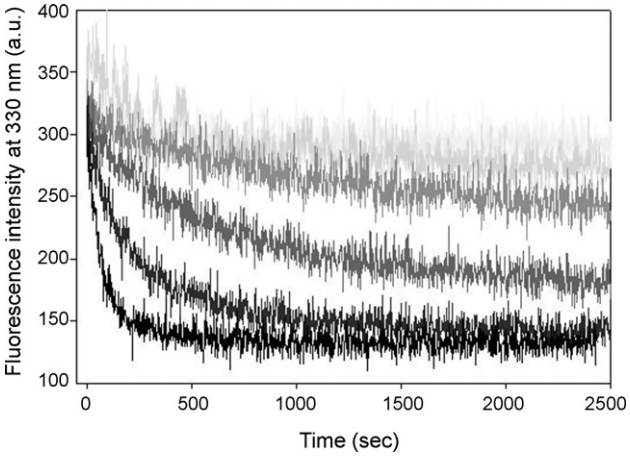

Fig. 3. Exponential decay of the fluorescence intensity at 330 nm from a rapid mixing of Cyt2Aa2 with various concentration of GuHCl. The faster (darker color) and slower (lighter color) decays were observed when using higher and lower concentrations of GuHCl, respectively.

intensity and a red shift of λ_{max} toward 350 nm (Fig. 1). The shifting of λ_{max} to a longer wavelength was similar to other reported unfolding proteins such as concanavalin A, methanol dehydrogenase, and glycyl-tRNA synthetase, indicating a conformational change of tryptophan residues from an apolar to a polar environment (Wang et al., 2000; Dignam et al., 2001; Chatterjee and Mandal, 2003). With a series of intensity ratio between 330 and 350 nm representing native and unfolded conformations, an unfolding curve was then established as a function of the denaturant (Fig. 2). The resulting curve demonstrated a well-defined feature corresponding to a three-state transitional model. These three revealed conformational states could be assumed to represent the native (N), intermediate (I) and unfolded states (U). This suggests that GuHCl could bind and help stabilize intermediate and unfolded conformations of the toxin. The steady-state conformations for N, I and U can be obtained at approximately 0–2, 3–4 and 6–7 M of GuHCl, respectively. Based on the three-state model equation, a curve fitting was performed which yielded values for denaturant concentration at a half unfolding ($[GuHCl]^{50\%}$) and transitional slope (m). These data were then used to determine the conformational free energy of protein in a denaturant-free condition (ΔG_w). After a number of independent repeats, we could report a conformational free energy of the native state at 5.82 ± 0.47 kcal/mol, while the free energy of the intermediate against the fully unfolded state was 16.85 ± 1.47 kcal/mol. The reverse process of these conformational changes was also analyzed by a refolding experiment. Interestingly, the derived refolding curve and free energy values were found to be very similar to those obtained from the unfolding study. These results confirmed that the two investigated pathways are simply a reversal process of the same route and existing conformations. When considering the completed transition, starting from native to unfolded state, the summation of conformational free energy found for Cyt2Aa2 toxin was 22.67 ± 1.94 kcal/mol. This total unfolding free energy was comparable to the stabilizing energy of other native proteins with a similar molecular weight, as reported in the database (Gromiha et al., 1999), such as 25-kDa glutathione S-transferase, 21-kDa γD crystallin, and 28-kDa β-lactamase (Vanhove et al., 1997; Hornby et al., 2000; Flaugh et al., 2005). These proteins undergo a three-state unfolding involving 12–27 kcal/mol of free energy. Moreover, the total unfolding free energy for Cyt2Aa2 toxin was also found to be similar to the previously reported data from the two-state unfolding of *B. thuringiensis* Cry4Ba toxin (Krittanai et al., 2003).

3.2. Kinetics of unfolding and activation energy analysis

In order to investigate the kinetics among these identified conformational states, a rapid mixing of purified toxin in carbonate buffer with various GuHCl concentrations was performed. During the mixing, intensity changes of fluorescence emission spectra were monitored over a period of time, as shown in Fig. 3. The emission intensity corresponding to the native state at 330 nm was found to decrease obviously and rapidly after the addition of a denaturant. In addition, a more significant change of 330-nm intensity was repeatedly obtained when using a higher concentration of GuHCl. Based on the first order of single exponential equation, we were able to obtain an apparent rate constant (k_{obs}) for each denaturant condition. A linear plot between $\ln k_{obs}$ and GuHCl concentrations provided rate constants in a denaturant-free condition (k_w) of 3.62×10^{-6} and 5.83×10^{-10} s^{-1} for the first and second transitions. Then the activation energy ($E_{ac,w}$) for these two transitions was finally obtained: 23.10 ± 0.28 and 24.89 ± 0.10 kcal/mol, respectively. Despite the activation energy for both transitions being very similar, the rate constant of the second transition was much slower than that of the first one. Thus this transition from an intermediate to an unfolded state could be identified as a rate-limiting step of the unfolding pathway.

3.3. Construction of an energy map

The combined data from steady-state and kinetic analyses can provide necessary information for the construction of a conformational energy map of the unfolding toxin. Conformational free energy (ΔG_w) of the three conformational states together with the activation energy ($E_{ac,w}$) of both transitions were mapped along the pathway progression, as shown in Fig. 4. This energy map displays an unfolding pathway starting from a lower-energy native state, and proceeding to higher-energy intermediate and unfolded states, respectively. The transition between each conformational state involves thermodynamic free energy around 5 and 16 kcal/mol, and activation energy around 23–24 kcal/mol. This energy map for the Cyt toxin family was experimentally established for the first time in this study. It could provide relative energy characteristics for the study of protein structure and stability, and could be used as a reference for structural engineering of the mutant toxins.

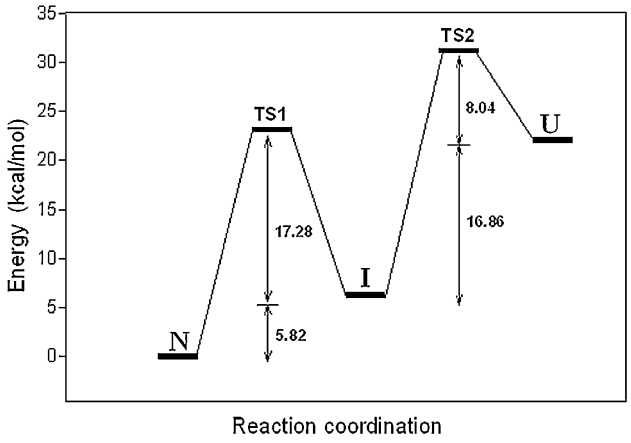

Fig. 4. The energetic map of Cyt2Aa2 unfolding/refolding, showing the relative energy levels for native (N), intermediate (I) and unfolded (U) states. The activation energy was also labeled for each conformational transition.

3.4. Characterization of intermediate state

ANS binding assay was applied to probe for an exposure of the protein hydrophobic core upon a conformational change. When fluorescent dye binds to the toxin, its emission spectrum is experimentally established with a λ_{max} of 465 nm. When this assay was performed for each denaturing condition, the results showed the maximal intensity of binding when the toxin was in 3.0–3.5 M GuHCl. It is apparent that the adopted intermediate state in this denaturing condition has a relaxed structure, and extensively exposes its hydrophobic core to the environment. We also analyzed the secondary structure of the toxin using circular dichroism spectroscopy. The CD spectra obtained for the native, intermediate and unfolded states are shown in Fig. 5. Interestingly, while the CD spectrum for the unfolded state indicated a significant loss of protein secondary structure, the spectra for the intermediate and native states were found to be very similar. This result suggested that the same secondary structure element is maintained in both native and intermediate states. In addition, our intrinsic fluorescence data for the intermediate state showed a red shift of λ_{max} toward 340 nm, indicating a detectable loss of the toxin's tertiary structure. Taking these data together, we were able to demonstrate that the intermediate state was present as a loose folding of the native-like secondary structure and the exposed hydrophobic core. Thus, this stable intermediate can be characterized molten globule state.

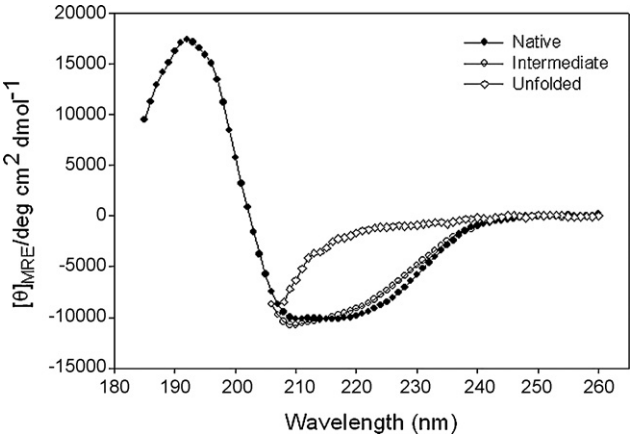

Fig. 5. Circular dichroism spectra of Cyt2Aa2 toxin in the native, intermediate and unfolded states. Purified toxin of 0.3 mg/ml was applied, and the spectra expressed in $[\theta]_{MRE}$/deg cm^2 dmol^{-1}.

Several reports on the protein folding pathway (Goldberg et al., 1990; Ptitsyn et al., 1990; Sugawara et al., 1991) involve a molten globule state formation. Moreover, the molten globule states for diphtheria toxin (Chenal et al., 2002), anthrax protective antigen (Gupta et al., 2003) and colicins (Zakharov and Cramer, 1997) had been shown to be responsible for their functions in protein–lipid membrane interactions. For *B. thuringiensis* toxin, a molten globule has been proposed for Cyt1A toxin in the presence of liposome vesicles, using differential scanning calorimetry and CD spectroscopy (Butko et al., 1997). The toxin binds and releases the dye from lipid membrane vesicles at low pH (Butko et al., 1996, 1997). It has been proposed that the molten globule structure binds to the lipid membrane independent from the net charge of the membrane. The importance of a molten globule for biological functions could also be inferred for Cyt2Aa2. Our data directly suggest a presence of molten globule in its unfolding and refolding pathway. When the native and intermediate states of the toxin are related in terms of mechanism of action, it is clear that the native conformation is required for the production of toxin, providing a stable form of protease resistance. However when the toxin undergoes a proteolytic activation and conformational change, a formation of molten globule could then be required for an active role in toxin and membrane interaction. Future investigation of the functional role and interacting mechanism of the intermediate revealed in this work could help provide a basic understanding of the toxin structure as well as a better mechanism model to be used for the application of Cyt2A toxin.

Acknowledgements

This work was supported by the Thailand Research Fund (TRF) and the Thailand Center of Excellence for Physics (Integrated Physics Cluster). Graduate Scholarships from the Commission on Higher Education Staff Development program to A.S. and the Thailand Graduate Institute of Science and Technology (TGIST) to W.T were gratefully acknowledged.

References

Andrews, R.E., Bibilos, M.M., Bulla, L.A., 1985. Protease activation of the entomocidal protoxin of *Bacillus thuringiensis* subsp. *kurstaki*. Appl. Environ. Microb. 50, 737–742.

Armstrong, J.L., Rohrmann, G.F., Beaudreau, G.S., 1985. Delta endotoxin of *Bacillus thuringiensis* subsp. *israelensis*. J. Bacteriol. 161, 39–46.

Bulla, L.A., Kramer, K.J., Davidson, L.I., 1977. Characterization of the entomocidal parasporal crystal of *Bacillus thuringiensis*. J. Bacteriol. 130, 375–383.

Butko, P., Huang, F., Pusztai-Carey, M., Surewicz, W.K., 1996. Membrane permeabilization induced by cytolytic delta-endotoxin CytA from *Bacillus thuringiensis* var. *israelensis*. Biochemistry 35, 11355–11360.

Butko, P., Huang, F., Pusztai-Carey, M., Surewicz, W.K., 1997. Interaction of the δ-endotoxin CytA from *Bacillus thuringiensis* var. *israelensis* with lipid membranes. Biochemistry 36, 12862–12868.

Butko, P., 2003. Cytolytic toxin Cyt1A and its mechanism of membrane damage: data and hypotheses. Appl. Environ. Microb. 69, 2415–2422.

Chatterjee, A., Mandal, D.K., 2003. Denaturant-induced equilibrium unfolding of concanavalin A is expressed by a three-state mechanism and provides an estimate of its protein stability. Biochim. Biophys. Acta 1648, 174–183.

Chenal, A., Savarin, P., Nizard, P., Gillet, D., Forge, V., 2002. Membrane protein insertion regulated by bringing electrostatic and hydrophobic interaction into play: A case study with the translocation domain of diphtheria toxin. J. Biol. Chem. 277, 43425–43432.

Dignam, J.D., Qu, X., Chaires, J.B., 2001. Equilibrium unfolding of *Bombyx mori* glycyl-tRNA synthetase. J. Biol. Chem. 276, 4028–4037.

Flaugh, S.L., Kosinski-Collins, M.S., King, J., 2005. Contributions of hydrophobic domain interface interactions to the folding and stability of human gamma D-crystallin. Protein Sci. 14, 569–581.

Galjart, N.J., Sivasubramanian, N., Federici, B.A., 1987. A plasmid location, cloning, and sequence analysis of the gene encoding a 27 3-kilodalton cytolytic protein from *Bacillus thuringiensis* subsp. *morrisoni* (PG-14). Curr. Microbiol. 16, 171–177.

Goldberg, M.E., Semisotnov, G.V., Friguet, B., Kuwajima, K., Ptitsyn, O.B., Sugai, S., 1990. An early immunoreactive folding intermediate of the tryptophan synthease beta 2 subunit is a 'molten globule'. FEBS Lett. 263, 51–56.

Gromiha, M.M., An, J., Kono, H., Oobatake, M., Uedaira, H., Sarai, A., 1999. ProTherm: thermodynamic database for proteins and mutants. Nucleic Acids Res. 27, 286–288.

Gupta, P.K., Kurupati, R.K., Chandra, H., Gaur, R., Tandon, V., Singh, Y., Maital, K., 2003. Acidic induced unfolding of anthrax protective antigen. Biochem. Biophys. Res. Commun. 311, 229–232.

Hofte, H., Whiteley, H.R., 1989. Insecticidal crystal proteins of *Bacillus thuringiensis*. Microbiol. Mol. Biol. Rev. 53, 242–255.

Hornby, J.A., Luo, J.K., Stevens, J.M., Wallace, L.A., Kaplan, W., Armstrong, R.N., Dirr, H.W., 2000. Equilibrium folding of dimeric class mu glutathione transferases involves a stable monomeric intermediate. Biochemistry 39, 12336–12344.

Ibarra-Molero, B., Sanchez-Ruiz, J.M., 1996. A model-independent, nonlinear extrapolation procedure for the characterization of protein folding energetics from solvent-denaturation data. Biochemistry 35, 14689–14702.

Krittanai, C., Bourchookarn, A., Pathaichindachote, W., Panyim, S., 2003. Mutation of the hydrophobic residue on Helix 5 of the *Bacillus thuringiensis* Cry4B affects structural stability. Protein Peptide Lett. 10, 361–368.

Li, J., Koni, P.A., Ellar, D.J., 1996. Structure of the mosquitocidal δ-endotoxin CytB from *Bacillus thuringiensis* sp. *kyushuensis* and implication for membrane pore formation. J. Mol. Biol. 257, 129–152.

Murphy, D.W., Sohi, S.S., Fast, P.G., 1976. *Bacillus thuringiensis* enzyme-digested delta endotoxin: effect on cultured insect cells. Science 194, 954–956.

Nickerson, K.W., De Pinto, J., Bulla, L.A., 1975. Lipid metabolism during bacterial growth, sporulation, and germination: kinetics of fatty acid and macromolecular synthesis during spore germination and outgrowth of *Bacillus thuringiensis*. J. Bacteriol. 121, 227–233.

Nozaki, Y., 1972. A preparation of guanidine hydrochloride. Methods Enzymol. 26, 43–50.

Promdonkoy, B., Ellar, D.J., 2000. Membrane pore architecture of a cytolytic toxin from *Bacillus thuringiensis*. Biochem. J. 350, 275–282.

Promdonkoy, B., Chewawiwat, N., Tanapongpipat, S., Luxananil, P., Panyim, S., 2003. Cloning and characterization of a cytolytic and mosquito larvicidal delta-endotoxin from *Bacillus thuringiensis* subsp *darmstadiensis*. Curr. Microbiol. 46, 94–98.

Promdonkoy, B., Ellar, D.J., 2003. Investigation of the pore-forming mechanism of a cytolytic delta-endotoxin from *Bacillus thuringiensis*. Biochem. J. 374 (Pt 1), 255–259.

Ptitsyn, O.B., Pain, R.H., Semisotnov, G.V., Zerovnik, E., Razgulyaev, O.I., 1990. Evidence for a molten globule state as a general intermediate in protein folding evidence for a molten globule state as a general intermediate in protein folding. FEBS Lett. 262, 20–24.

Schnepf, E., Crickmore, N., Van Rie, J., Lereclus, D., Baum, J., Feitelson, J., Zeigler, D.R., Dean, D.H., 1998. *Bacillus thuringiensis* and its pesticidal crystal proteins. Microbiol. Mol. Biol. Rev. 62, 775–806.

Sugawara, T., Kuwajima, K., Sugai, S., 1991. Folding of staphylococcal nuclease A studied by equilibrium and kinetic circular dichroism spectra. Biochemistry 30, 2698–2706.

Thomas, W.E., Ellar, D.J., 1983. *Bacillus thuringiensis* var *israelensis* crystal delta-endotoxin: effects on insect and mammalian cells in vitro and in vivo. J. Cell Sci. 60, 181–197.

Vanhove, M., Guillaume, G., Ledent, P., Richards, J.H., Pain, R.H., Frere, J.M., 1997. Kinetic and thermodynamic consequences of the removal of the Cys-77-Cys-123 disulphide bond for the folding of TEM-1 beta-lactamase. Biochem. J. 321, 413–417.

Waddell, W.J., 1956. A simple ultraviolet spectrophotometric method for the determination of protein. J. Lab. Clin. Med. 48, 311–314.

Wang, G.F., Cao, Z.F., Zhou, H.M., Zhao, Y.F., 2000. Comparison of inactivation and unfolding of methanol dehydrogenase during denaturation in guanidine hydrochloride and urea. Int. J. Biochem. Cell Biol. 32, 873–878.

Zakharov, S.D., Cramer, W.A., 1997. Insertion intermediates of pore-forming colicins in membrane two-dimension space. Biochemistry 36, 12862–12868.